

PAPER • OPEN ACCESS

## Quasi-tomography by free space line field spectral domain optical coherence reflectometry

To cite this article: Samuel Lawman *et al* 2020 *Meas. Sci. Technol.* **31** 065203

View the [article online](#) for updates and enhancements.

You may also like

- [Comprehensive study on the concept of spectral-domain reflection and refraction](#)  
Chunxiang Zhang, Zhixiang Deng, Yu Chen et al.
- [Bayesian inference using JET's microwave diagnostic system](#)  
S. Schmuck, J. Svensson, L. Figini et al.
- [Two-dimensional correlation analysis for x-ray photoelectron spectroscopy](#)  
S Li, T Driver, A Al Haddad et al.

# Quasi-tomography by free space line field spectral domain optical coherence reflectometry

Samuel Lawman<sup>1,2</sup> , Bryan M Williams<sup>2</sup>, Yalin Zheng<sup>2</sup> and Yao-chun Shen<sup>1</sup>

<sup>1</sup> Department of Electrical Engineering and Electronics, University of Liverpool, Liverpool, United Kingdom

<sup>2</sup> Department of Eye and Vision Science, University of Liverpool, Liverpool, United Kingdom

E-mail: [Y.C.Shen@liverpool.ac.uk](mailto:Y.C.Shen@liverpool.ac.uk)

Received 5 August 2019, revised 25 November 2019

Accepted for publication 3 February 2020

Published 17 March 2020



CrossMark

## Abstract

This paper reports the development of a new technique, free space line field spectral domain optical coherence reflectometry (LF-SD-OCR), which is able to produce tomographic like (quasi) images. Furthermore, the capabilities and cost benefits of the technique are demonstrated by constructing a handheld LF-SD-OCR device. For glossy paint systems and other suitable samples, the line field format produces quasi-tomographic (cross-sectional) imaging through the layers, with axial and lateral image resolutions of 1.3  $\mu\text{m}$  and 40  $\mu\text{m}$  respectively. From these, the clear coat thicknesses on the bonnet of cars were measured by graph search segmentation and maximum A-scan projection. In comparison with the widely used single point ultrasound and optical devices, our technique gives the user more confident interpretation of the results as it produces a cross-sectional image of the sample in a single-shot fashion without the need of any mechanical scanning. In addition, the produced device has higher resolution and lower cost (£1660 cost of the constructed one-off prototype as compared with over £10K for comparable universally capable ultrasonic devices), making the technique an economically viable alternative to ultrasound in the quality assurance of coating systems and other application areas such as plastic film manufacturing control.

Keywords: spectral domain reflectometry, optical coherence tomography, industrial coating quality assurance

(Some figures may appear in colour only in the online journal)

## 1. Introduction

In order to obtain the correct aesthetics and sufficient protection, multi-layer coating systems are widely used in industry [1], particularly in the automotive industry [2]. For quality assurance [3, 4], in product manufacture or repair of coating systems, consistent thickness of the applied layers needs to

be ensured. This requires suitable tools [5] to measure layer thicknesses. Magnetic induction and eddy current probes cost less than £100; however, they only work on metallic substrates and are limited to measuring only total coating thickness, giving no information on thicknesses of the individual layers in multi-coating systems. The current gold standard for coating thickness measurements are ultrasonic-based devices, although their capabilities vary significantly with price. These systems measure the time taken for sound waves to be reflected from different coating interfaces, giving (assuming prior knowledge of the speed of sound in each material) the potential for thickness measurements to be taken from multiple layers on the majority of coating-substrate systems. Ultrasonic



Original content from this work may be used under the terms of the [Creative Commons Attribution 3.0 licence](https://creativecommons.org/licenses/by/3.0/). Any further distribution of this work must maintain attribution to the author(s) and the title of the work, journal citation and DOI.

devices capable of measuring layered coating on non-metallic substrates can be purchased for around £1800 [6, 7] (as of a product search in July 2019). However, these devices can only measure total thickness of coatings when on metallic substrates, so are not a universal solution to measure coating layer thicknesses. The cost of devices that can measure individual layer thickness on all substrates is >£10 000 [8, 9]. The majority of devices on the market necessitate contact with the sample being measured, usually with a sonic coupling liquid or gel; non-contact [10] systems do exist but this further increases the cost and complexity. Ultrasonic devices are limited by axial image resolution to a minimum resolvable layer thickness of around 10  $\mu\text{m}$ . Note this is not the same as precision (repeatability) and accuracy (error) of the measured thickness values, which in some scenarios can be found up to orders of magnitude smaller (e.g. [11, 12]) than axial image resolution but are often (erroneously for an imaging context) labelled as resolution.

Optical coherence tomography (OCT) is a high-resolution tomographic imaging technique that has multiple applications in the coating field [12, 13], including measurement of flake statistics [14], dryness and surface texture [12], on top of layer thicknesses [15]. The technique is analogous to ultrasound, but instead measures the time delay of light reflections and scattering from within the sample, relative to an engineered reference path (by coherence interferometry). Axial distances can be calculated with prior knowledge of materials group refractive index. In spectral domain (SD) OCT, although image signals can be generated by self-interference of the light from the sample only, they are generally disregarded and treated as an unwanted artefacts. The axial and lateral resolution of SD OCT systems are commonly of the order of a few microns. Though much more versatile than thickness measurement probes, this comes at a cost with the market price of OCT systems generally >£10 000 [16]. One method to reduce cost is to use a line field spectral domain setup, removing the need for mechanically moving parts to obtain a tomographic image [15]. However this setup still had relatively expensive component cost, including requiring a separate reference path for the interferometer and a relatively expensive light source. Reducing the cost of OCT-based technology, to measure individual coating layer thicknesses for a lower cost, more confident interpretation and a higher resolution, than by the current ultrasound devices, would be of economic and commercial interest in the automotive sector. Similar interest in methods to lower the cost of OCT technology exists for applications in other fields as well [17–20].

Closely related to SD-OCT, SD-optical coherence reflectometry (SD-OCR) [21] is widely used in the thin film industry (e.g. Filmetrics' devices [22]) to measure thicknesses of layers down to a few nanometres. The physics this technique is built on is identical to SD-OCT (i.e. spectrally resolved broadband interference) but how the measurement data is taken and used is different. In contrast to OCT, SD-OCR does not use a separate reference path, relying instead solely on the self-interference between different reflections of the sample. The signal may be initially Fourier transformed to identify coarse layer thicknesses [22] but precise measurement of thicknesses,

and resolution of layers thinner than optical coherence length [23], is generally done by fitting a simulated interference signal to the raw measured data. Currently, SD-reflectometry is not commonly used for industrial coatings. To the authors' knowledge, SD reflectometry has only previously been done in single (scanning) point (or laterally unresolved equivalent) systems.

A technique that is more widely used in (non-high-tech) industry, which is similar in practice to SD-OCT and SD-OCR but not in its underlying physics, is chromatic confocal microscopy [24]. This uses a deliberately chromatic objective, with the light returned measured by a spectrometer and wavelength mapping directly to the depth (after correction with prior knowledge of materials phase refractive index) of signal. This technique can be improved further by hybridisation with SD-OCT technology (meaning approximate true thickness and refractive index can be measured with no prior knowledge) [25, 26]. Note the device presented in this paper uses full field, instead of confocal, illumination, so does not fit into this category.

Similarly to SD-OCR, the most common setup for resolving the image laterally in OCT are scanning point systems, making use of compact and flexible fibre optics but requiring galvo mirrors or other mechanical scanning mechanisms to take an image. However, parallel measurement of lateral positions, which do not require any mechanical lateral or axial scanning mechanism to acquire tomographic images, is possible for 2D tomography with line field SD-OCT [15, 27] or even 3D volumes with full field swept source [28, 29] or 3D to 2D mapping SD OCT [30]. Here, we can take the line field SD format from SD-OCT and apply it to SD-OCR to remove the need for scanning mechanics to acquire 2D cross-sectional data. Such a system is novel, with the concept being disclosed by the authors in a patent application [31].

With this novel LF-SD-OCR setup, for the application to measure car paint systems, and other similar ones such as plastic film production, we make use of smooth glossy surfaces (as exists for the vast majority of automotive coatings), which provide a quasi-reference to form an image in the same way as SD-OCT. In addition, as there is no need for sample and reference beam recombination, the method can be done at a non-normal angle incidence/reflection, removing the requirement for any beam splitter like optics to separate illumination and imaging parts of the device. In this paper, we present such a low cost (approximate £1660 material cost for prototype device, with expectation that it could be reduced to approximately £1000) line field system, that is physically SD-OCR, but process the measured spectra as SD-OCT to form quasi-tomographic images [31]. The term quasi is important as the device does not produce true tomographic images of absolute locations. For the car paint system results presented in this paper, relative (to the surface interface) tomographic images are produced that are very close to the real tomographic images, only being distorted by the shape of the surface. Samples without a significant reflective interface would not produce any significant images, while samples with multiple strong reflective interfaces (e.g. a stack of films with air gaps) would produce a complex superposition of relative

images, which would have to be interpreted. The authors are not aware of any other published SD-OCR system that is designed specifically to produce quasi-tomographic images. From these images, layer thickness can be measured. The device is designed to work at  $45^\circ$  reflection from the sample. Using this prototype handheld device, we demonstrate the method is practical for real world use by the validation against conventional LF-SD-OCT on test samples, and the measuring of clear coat thickness of real cars.

## 2. Device and methods

Figure 1(a) shows a diagram of the LF-SD-OCR device. The optics were mounted and contained in a custom white selective laser sintered 3D printed case. Key optical areas of the case were optically blacked out to allow the device to work in room light. The case also served as a physical contact spacer to position the car paint surface at the correct position. The light source is a 1 W white LED (MWWHL3, Thorlabs), mounted behind a 4 mm diameter aperture that is part of the case. Light passing through the aperture was collimated by an  $f = 100$  mm singlet lens (LA1509-A-ML, Thorlabs). Though counter intuitive, due to low optical efficiency, this spot light illumination has two benefits. Firstly, the illuminated area is large in comparison to the source, intrinsically increasing spatial coherence. This effect has been observed by us experimentally, that spot light illumination (Kohler Illumination) is much more tolerant in system alignment to be able to produce interference with a high coherence factor, than when imaging the light source onto the sample (Critical Illumination). It can be also simulated numerically. The location of the sample is approximately on the Fourier plane (of light source and illuminating lens), so statically we can simulate a complex field of small area and small spatial coherence (i.e. complex values of pixels are random and independent, the degree of spatial coherence can be moderated by starting with a grid of random complex values and interpolating values between), the values outside the small area are set to zero. Taking the 2D FFT of this field, in the larger illuminated the spatial coherence distances of phase angle and amplitude are visually larger. Making an analogy with spatial modes in optical fibres, the amount of discrete truly independent (incoherent) locations has stayed approximately the same, but they are spread over a larger area. Secondly, the wide area illumination means that test objects that are not perfectly aligned, likely to be a common occurrence in real use, still result in light onto the slit and give a result. Overall the device was designed to be resilient to sample alignment. The light reflection from the sample surface and substructure was imaged onto a  $10\ \mu\text{m}$  slit (S10RH, Thorlabs) by a 50–75 mm achromatic lens pair (MAP105075-A, Thorlabs). The light entering the slit of the custom spectrograph was collimated by a 30 mm achromatic doublet lens (AC254-030-A-ML, Thorlabs).

The grating of the spectrograph was negligible cost roll printed film, 1000 lines/mm (#40-267, Edmund Optics). The imaging lens of the spectrograph was a 50 mm achromatic doublet (AC254-050-A, Thorlabs). A  $5.86\ \mu\text{m}$  pixel CMOS camera (BFLY-U3-23S6M-C, FLIR) was used for detection,

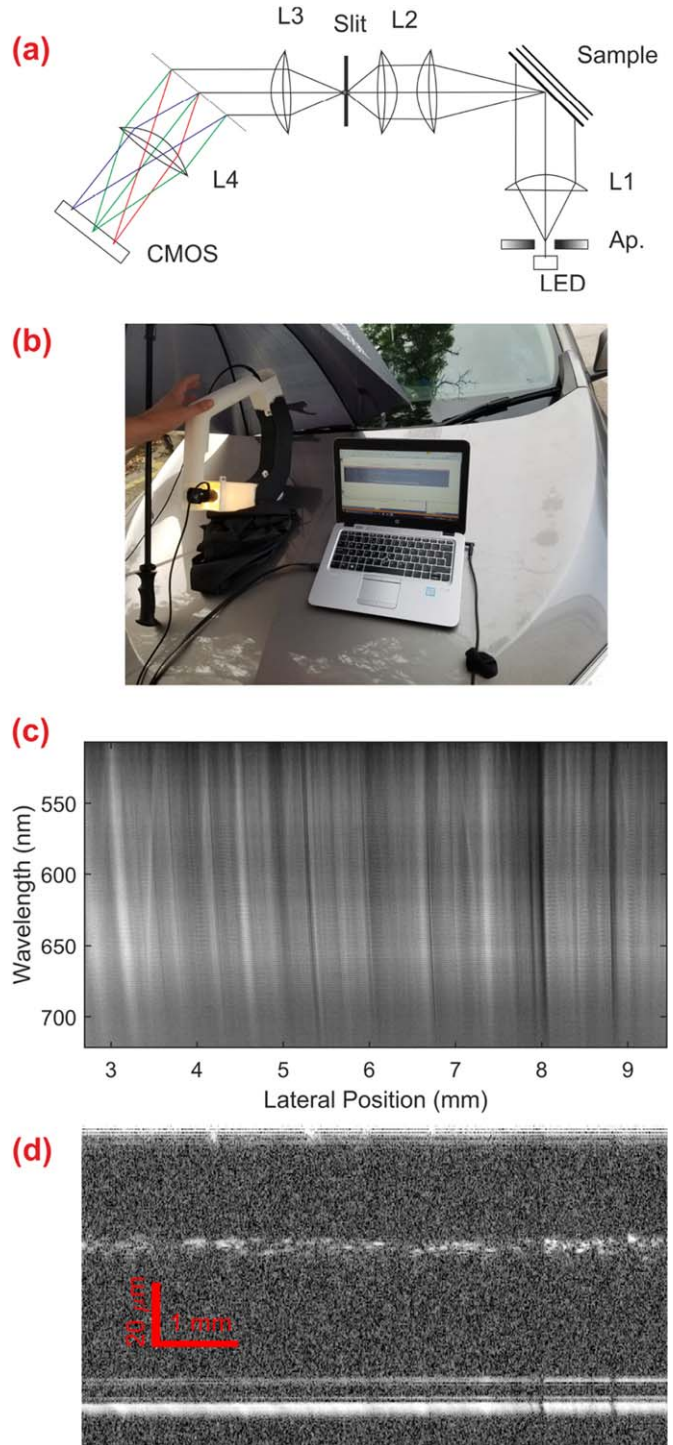


**Figure 1.** (a) Diagram of LF-SD-OCR system. LED—white LED light source, Ap.—4 mm diameter aperture, L1—Singlet collimation lens, L2—Achromatic doublet pair, L3—Achromatic double spectrograph collimation lens, L4—Achromatic double spectrograph imaging lens. CMOS—FLIR USB 3.0 camera. (b) Photograph of LF-SD-OCR device in use on car. (c) Raw image data from the camera. (d) Resultant un-averaged image after resampling, windowing and FFT in wavelength dimension.

with an integration time of 0.5 s due to the tiny fraction of total light transmitted through the slit. The device was connected to a laptop. Figure 1(b) is photograph of the device in use on a car.

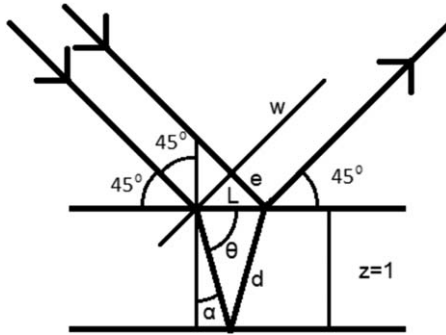


**Figure 2.** Diagram for the calculation of angled OCR scaling factor relative to normal incidence OCT in air.

Data acquisition, live quasi-tomographic image display and data capture was done with custom software written in C++ (and C++/CLI for GUI elements) (Microsoft Visual Studio 2013 Community Edition). For the live image display, after image acquisition (figure 1(c)) the image data was resampled in equal frequency space. A Tukey window was applied, mainly to reduce ringing from the DC signal. Each A-Scan was fast Fourier transformed (KissFFT 1.3), the magnitude taken and converted to dB (figure 1(d)). For the further results presented, the device was positioned using live view before the capture of 15 raw images was initiated by pressing a key on the laptop. These recorded images were processed afterwards (in MATLAB) in the same method as the live display images with the addition of the average of the 15 frames being taken after the magnitude of the Fourier transform is taken, but before conversion of the averaged image to dB.

The processing of the quasi-tomographic LF-SD-OCR images is identical to SD-OCT, as such the axial axis scaling is calculated as normal incidence OCT ( $n = 1$ ) and then corrected with a scaling factor dependent on the sample refractive index. As OCT directly measures information delay and measures directly backscattered or reflected light, axial distance scaling inside a material has to be corrected (relative to air or vacuum) by dividing by the materials group refractive index. However, as this LF-SD-OCR device is measuring the target at a reflection angle of  $45^\circ$ , the calculation of axial scaling is more complicated due to the angled direction of travel of light relative to the samples axial direction, refraction and relative lateral shifting of wave front reflected from different depths. Figure 2 shows a diagram of light rays incident on a sample. ‘W’ shows a wave front (i.e. line of equal phase) of this light as it is incident on the sample. As we are calculating just the scaling, the real axial distance,  $z$ , is set to unity. The two rays shown are picked to superimpose after reflection. In this derivation, the approximation of phase and group refractive index being equal is made. From Snell’s law,  $\alpha$  can be calculated to be

$$\sin(\alpha) = \frac{\sin(45)}{n}$$

$\theta$  can be calculated

$$\theta = 90 - \alpha$$

The physical length,  $d$ , is given by

$$d = \frac{z}{\sin(\theta)} = \frac{1}{\sin(\theta)}$$

The physical length,  $L$ , is given by

$$L = \frac{2}{\tan(\theta)}$$

The extra distance travelled by the ‘reference’ ray in air can be calculated by

$$e = L \sin(45)$$

The extra physical distance that the ‘measured’ ray travels is  $2d$ . However, the apparent distance travelled (relative to in air or a vacuum) is multiplied by  $n$ . Hence, it becomes  $2dn$ . As the real distance travelled by light measuring the sample at normal incidence would be 2 (forwards + backwards), the scaling factor for this LF-SD-OCR system is given by

$$S = \frac{2}{2dn - e}$$

From the above derivation, a source of potential error can be identified. The prototype device presented here has been designed to be tolerant of alignment to the sample, to allow ease of use. If the device does not sit flush with the sample, an error of 5 degrees would lead to an error of the scaling factor of up to 2.7%. Likewise, a curved surface would be expected to lead to similar source of errors, however the variation in angles due to curvature, at locations practical to be measured with the presented prototype, would lead to negligible angle variation in comparison.

Depending on the amount of signal from the base coat layers, the thickness was extracted in two ways. For both test sample and silver car measurements, where the signal was continuous, the graph search method detailed in [15, 32, 33] was used to measure clear coat thickness. OCR quasi-tomography is a simplification from its use in OCT, as the surface is always the top of the image so does not have to be found, and sample shape and orientation does not matter to the location of the desired signals in the image.

For measurements where the signal from the base coat was sparse, as occurred for the black car measurements, a maximum projection A-scan is taken across the B-Scan. As the top of the image is the surface, sample orientation and shape does not have to be taken into account, unlike in conventional OCT images. A manual method to assess thickness was derived using the paint sampler data where image quality was sufficient for segmentation, even for black.

To quantify axial resolution and demonstrate another application area, the measurement of plastic film thickness, a bubble wrap sample (assumed material LDPE) was measured with the LF-SD-OCR device. From the interface signal, the axial resolution was quantified by fitting a Gaussian point spread function. To measure the lateral resolution, the engraved rulings of a metal ruler were measure with the device.

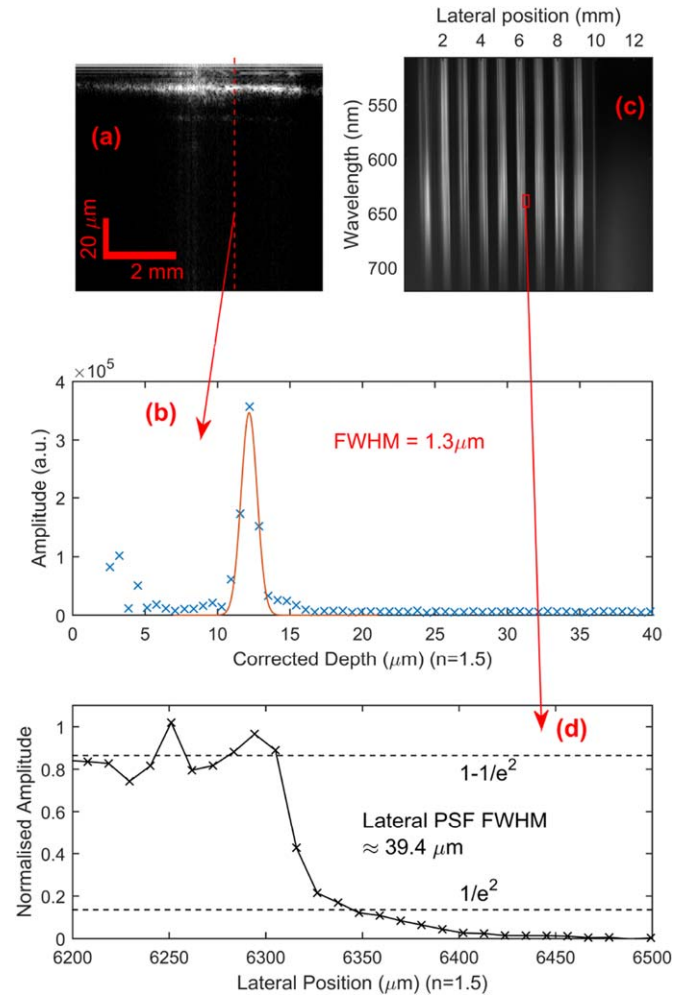
From the raw image data of this edge, the device's lateral imaging PSF FWHM resolution was measured.

To validate coating thickness measured by the LF-SD-OCR, we measured two paint system samples Indus silver and Santorini black with the device and a new unpublished LF-SD-OCT system that has been developed following our previous system [34]. The thickness of the clear coat of the both paint systems were measured with both instruments and compared. To demonstrate that LF-SD-OCR can be used for real world applications, the prototype LF-SD-OCR was used to measure clear coating thickness on two different cars. A silver Renault Megane and a black Ford C-max. For each car, multiple ( $N \geq 5$ ) measurements were taken on the bonnet of each car at random locations. For all samples, the refractive index of the clear coat was assumed to be 1.56 [13].

### 3. Results

Figure 3(a) shows the measurement result of bubble wrap film (assumed LDPE). The film thickness of approximately  $12 \mu\text{m}$ , is easily resolved. To measure the system's axial resolution, a clean A-Scan was selected (figure 3(b)), and a Gaussian PSF fitted to the interference peak. This gives an axial resolution of  $1.3 \mu\text{m}$  (in LDPE,  $n = 1.5$ ), for clean signals. Figure 3(c) shows the raw image data of the measurement of ruler rulings (nominally clean edges), with red box showing data presented in figure 3(d) for the measurement of lateral resolution of the device. The lateral distance for the normalised signal to fall from  $1-1/e^2$  to  $1/e^2$  (can be shown by numerical convolution simulation to correspond to approximately the FWHM of a Gaussian PSF) is approximately  $40 \mu\text{m}$ , which corresponds to 3.6 pixels at the camera. This is quite low lateral resolution for optical systems, mainly due to the purposely designed large lateral range of  $9.5 \text{ mm}$  (limited by slit length). Note that designing a LF-SD-OCR system to have higher lateral resolution down to a few microns, if required, should be straightforward.

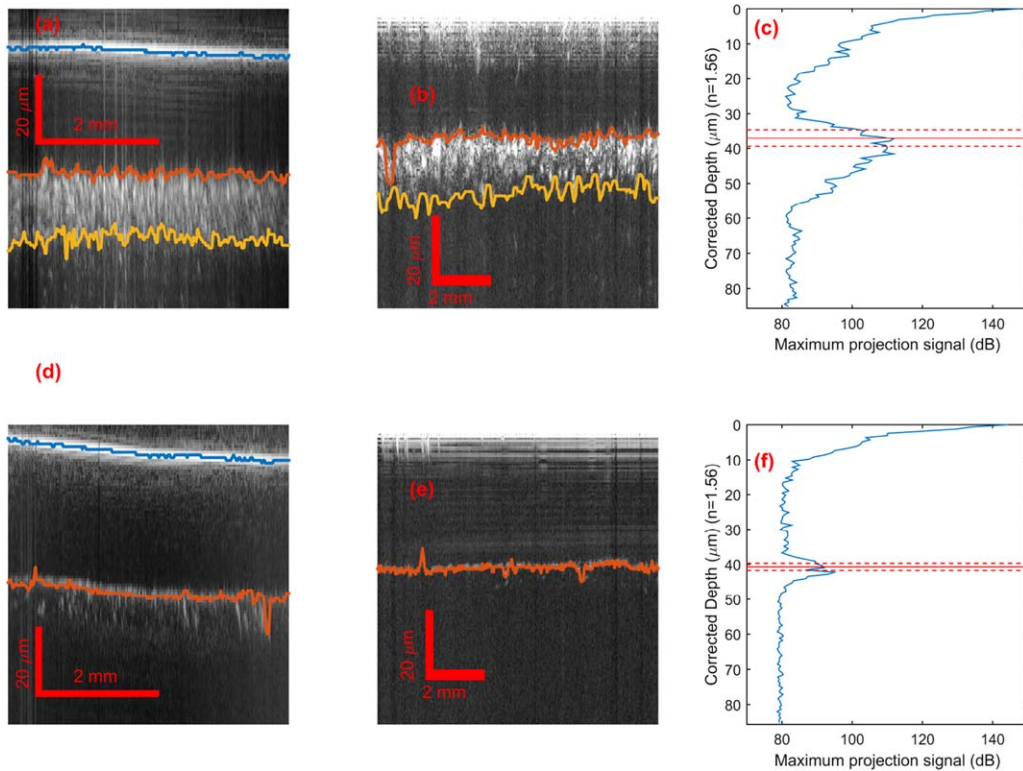
Figure 4(a) shows an LF-SD-OCT image of the Indus silver paint system sample. Note that the lower scattering layer in the image due to multiple reflections between the surface and base coat, and the high sensitivity of OCT. Figure 4(b) is the comparative quasi-tomographic image from the lower cost LF-SD-OCR system. Note that the air-clear coat interface is acting as the reference, so is at the very top of the image. The thickness of the clear coating can be extracted straightforwardly from both images by graph search segmentation. The thickness measured from these single independent measurements by LF-SD-OCR ( $37.6 \pm 2.4 \mu\text{m}$ ) and LF-SD-OCT ( $35 \pm 1.2 \mu\text{m}$ ) are a close match. Figure 4(d) (LF-SD-OCT) and (e) (LF-SD-OCR) are the same images for the Santorini black sample. Again, graph search segmentation can resolve the clear coat thickness of this sample in the lab. The clear coat thickness measured with LF-SD-OCR ( $41.3 \pm 1.0 \mu\text{m}$ ) is in reasonable agreement with the measurement by LF-SD-OCT ( $40.4 \pm 1.4 \mu\text{m}$ ). However, the reduced sensitivity of this low cost preliminary demonstration device for the LF-SD-OCR concept is apparent, with significantly less



**Figure 3.** (a) LF-SD-OCR image of bubble wrap film. Red dashed line shows the location of clean A-Scan shown in (b), with Gaussian fit to measure axial resolution. (c) Raw image of nominal clean edges (engraved ruling on metal ruler), with red box showing data shown in (d) for the estimation of the device's lateral imaging PSF resolution.

signal from the black base coat layer. Also, the use of visible light ( $507\text{--}721 \text{ nm}$ ) in the LF-SD-OCR device, compared with NIR light ( $700\text{--}950 \text{ nm}$ ) of the LF-SD-OCT system, may be a contributing factor. To demonstrate that LF-SD-OCT (figure 4(b)) can recover the thickness of multiple layers, the basecoat-primer interface was found (yellow line) with a modified (addition of threshold limiting of the image) segmentation method. This was compared with this interface found in the OCT image (yellow line, figure 4(a)). The thickness of the basecoat found by LF-SD-OCR was  $15.4 \pm 3.5 \mu\text{m}$ , compared to OCT of  $18.6 \pm 2.0 \mu\text{m}$ .

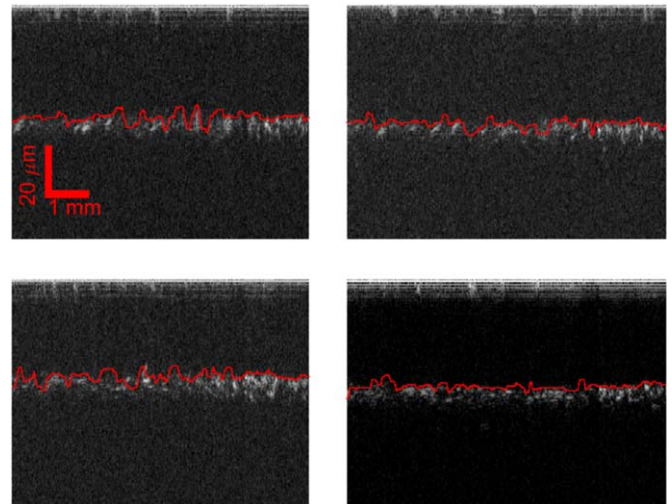
In the case of the measurement of a black car in a real world environment, presented below, the signal from the base coat was too discontinuous for graph search segmentation. In situations like this, where the signal is weak an alternative method is needed to quantify layer thickness from the image. This can be done by using a maximum projection A-Scan along the B-Scan direction, as the surface is the reference so image tilt is not an issue. The maximum projections of the LF-SD-OCR images for the Indus silver (figure 4(c))



**Figure 4.** LF-SD-OCT (a, d) and LF-SD-OCR quasi-tomographic (b, e) images and graph search segmentations of Indus silver (a, b, c) and Santorini black (d, e, f) paint system samples. (e, f) are maximum A-Scan projections along the OCR B-scan, the redlines show the mean  $\pm$  standard deviation thickness of clear coat from the graph search segmentation.

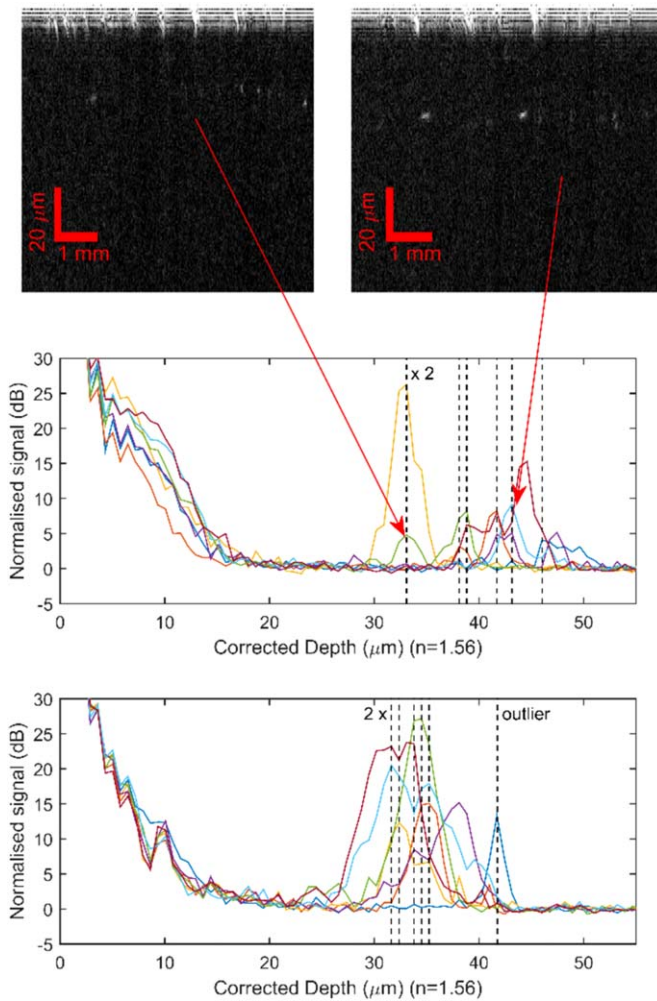
and Santorini black (figure 4(f)), shows that the mean profile thicknesses measured by graph search, correspond approximately to the front main peak of the maximum projection signal. This principle was used to subjectively manually estimate the thickness for the black car measurements below.

Figure 5 shows example quasi-tomographic images, taken with the LF-SD-OCR device, of the paint coatings of the silver Renault Megane. For all the measurements of the silver Renault Megane, the strong continuous signal from the base coat allowed the interface of the clear coat and base coat to be mapped by the graph search method. The segmentations for the example images are shown by the red lines in figure 5. From 5 measurements at different random locations on the bonnet the mean measured thickness of the clear coat on the silver Renault Megane was  $44.5 \mu\text{m}$  with the standard deviation between the mean thickness of each measurement was  $2.8 \mu\text{m}$  and the mean standard deviation of the thickness profiles of each measurement was  $1.7 \mu\text{m}$ . Beyond the quantitative, ultimately binary (pass or fail) output typically required of a quality assurance device, the tomographic image output of this device allows the operator a visual understanding of the measurement. This extra qualitative information (the image) may aid identification of failure causes quicker and more accurately than trying to interpret single point measurement data. A single image by this device also gives information over a  $9.5 \text{ mm}$  lateral range, giving information on local variance or features which would not be available by a single point measurement.



**Figure 5.** Four example LF-SD-OCR quasi-tomographic images, with graph search segmentations of clear coat—base coat boundary, taken with the prototype device on the bonnet of a silver Renault Megane.

The signal from the base coat of the black Ford C-Max (figure 6 (top)) was too dis-continuous to measure the clear coat thickness by graph search segmentation. It should be noted that black coloured paint systems are the worst case exception in the strength of signal from the base coat, with other colours having much stronger coherence interference signals from this layer [13, 15]. Also, this is only the first proof



**Figure 6.** Top left and right: Example quasi-tomographic images from two different locations on the bonnet of a black Ford C-Max, showing a visible difference in thickness of clear coat. Note image signal from base coat is too sparse for image segmentation. Instead, maximum A-scan projection of the seven repeat measurements (each) spread randomly over the whole (middle) and localised 50 × 50 mm area (bottom) of the bonnet of a black Ford C-max, along with the manually identified front peak for each. Where multiple lines overlay they are annotated, such as '2 x' with the 'x' nearest the line.

of concept prototype for LF-SD-OCR, with future refinements to the design of devices, the sensitivity of the technique is likely to increase, reducing the occurrence of this scenario. However, even in this scenario the clear coat thickness can still be measured by the maximum projection method. Figure 6 (middle) shows the maximum projection A-Scan of the base coat signal for 7 measurements at random locations over the whole bonnet, along with the manually identified front peak of the layer. From this method, the mean clear coat thickness measured was 39.1  $\mu\text{m}$  with a standard deviation of 4.9  $\mu\text{m}$ . This standard deviation corresponds to about 12.5% of the mean thickness, which is significant. Visual assessment of the raw quasi-tomographic images appeared to show genuine variation of clear coat thickness between the measurements. To confirm this was the case, the method was repeated but

this time keeping overall measurement area for the random measurements localised to an approximate 50 mm × 50 mm area. Figure 6 (bottom) shows the result, with the measured thicknesses showing far less deviation, excluding one outlier. The analysed image area for the outlier appears to contain just a single signal from the base coat layer, this signal appears to originate from bottom of the base coat signal. However, a single failure from 7 measurements is not debilitating to the application area (QA), where standard practice would expect the operator to take 3 repeat measurements then use the median. In these circumstances, the method would be reliable in the majority of cases. Excluding the outlier, the mean thickness is 33.2  $\mu\text{m}$ , so is a thinner area, with the standard deviation of 1.5  $\mu\text{m}$ . This variance is significantly reduced compared to the first set. So it is concluded that the variance in thickness measured over the whole bonnet is genuine.

#### 4. Discussion

In this paper, we have described the concept of free space LF-SD-OCR and demonstrated that it is a practical technique for real world measurement of clear coat thickness of automotive paint systems. As the technique is similar to OCT, this should also extend to the measurement of thickness of some base coats in future iterations of the technique. However, the main limitation of the presented technique, in comparison with ultrasound, will be the lack of ability to measure or measure through optically opaque layers. Our prior experience with the related technique OCT suggests primer coat and lower are not realistic targets for the technique, leaving only clear coat and some base coat layers that can be measured directly. For the relatively thin coatings and film measured in this study, interferometric roll off was a negligible problem in comparison, and was not measured. The combination of the technique with low cost eddy current and/or magnetic induction measurement of total thickness would recover some of this information. The purpose of this technique would be as a lower cost, higher resolution, alternative or addition to universal high-resolution ultra-sound systems. Table 1 lists and explains the potential advantages and disadvantages that LF-SD-OCR has in comparison to the industry standard high-resolution ultra-sound. To be a direct competitor to high resolution ultra-sound, LF-SD-OCR needs to be significantly lower cost. The total material cost at time of production was of £1660.85, meaning the device material costs are lower than buying a comparable ultra-sound system off the shelf. However given the disadvantages of larger size and less universality on the coatings it can measure, further reduction in cost is desirable to be an economically superior choice to ultra-sound for just the measurement of coating thicknesses. Over 50% of the cost of the device was made up of the chassis-case and camera. With increased manufacturing volume, instead of a single 3D print, the cost of the chassis-case would be reduced substantially. Similarly, the camera was chosen for convenience and availability in the lab; replacement with a lower cost CMOS detector should be possible. From this and other engineer-able savings, it should be reasonable to reduce the material cost

**Table 1.** Advantages and disadvantages of free space LF-SD-OCR in comparison to ultra-sound.

Advantages	Disadvantages
The imaging resolution of coherence quasi-tomography is intrinsically higher than ultra-sound	Though handheld, the size of free space LF-SD-OCR devices are unlikely to reduce down to the size of ultra-sound probes. This is an issue for hard to reach places
Quasi-tomographic images are achieved with LF-SD-OCR without the need for scanning or moving parts	The ability of optical methods to measure layer thickness is dependent on the optical opacity of that and preceding layers. However, the combining of LF-SD-OCR with magnetic induction or eddy current probe (in a single device), would overcome some of this while still maintaining low cost
LF-SD-OCR has lower cost and works independent of substrate	
Though this demonstration device was engineered to be contact to give easy alignment of the test object, the technology could be engineered into a non-contact device. For example, such a device could be used for the measurement coating dryness in an automotive paint workshop, utilising Fourier phase by the same method as given in [12]	

of a commercially manufactured version of this LF-SD-OCR device to around £1000, which would significantly distinguish the technique from comparable ultra-sound devices currently on the market. In addition to being a direct alternative to ultra-sound, LF-SD-OCR could find further applications due to its higher axial resolution and ability to measure coatings too thin to measure with ultra-sound or due to its intrinsic ability to be non-contact, e.g. for coatings or layers which are not in a solid state, including measuring coating dryness [12]. Away from automotive and industrial coatings, LF-SD-OCR could be applied to measure the thickness of other thin bodies, such as in the production of plastic film [35].

Ideally a direct experimental comparison of the technique with a similar custom-built high-resolution, high-frequency ultrasound system would be useful. However, the authors are not aware of any such 'home-built' ultrasound system, with suitable resolution, in the literature, and the construction of one would involve highly-specialised components and electronics. The overall cost for a one-off device not likely to be any less than commercial products available off the shelf. Contrasted to the presented LF-SD-OCR, where the demonstration device was constructed with common off the shelf components and a simple 3D printed case. For validation, for this application, between appropriate commercial high-resolution ultrasound and the presented technique, we have

previously cross-validated SD-OCT and ultrasound [8], and we have cross-validated different types OCT [10]. Therefore the behaviour and accuracy of OCT in this application is well known. Here we have validated LF-SD-OCR, against LF-SD-OCT, showing that LF-SD-OCR has very similar properties to any OCT technique, as expected.

To accurately quantify absolute thickness both ultrasound and all optical methods need prior knowledge of material properties. In ultrasound, the speed of sound through the material for the frequency of sound used needs to be known. In LF-SD-OCT, knowledge of the refractive index is required. This prior constraint is knowledge constraint is not onerous in quality assurance context for the following two arguments: (1) The materials used are going to be consistent and either their properties will be already well known, or easily measured by standard laboratory techniques (e.g. Abbe refractometer), beyond an accuracy that will have a significant impact of the accuracy of the technique. (2) Even without accurate prior knowledge of material properties, relative thickness measurement vs a pre-set target range would be sufficient as a quality control measure.

## 5. Conclusion

This paper has introduced quasi-tomography by the novel technique of free space LF-SD-OCR and demonstrated that it is a practicable technique to measure coating thicknesses in a real-world environment. For automotive coatings, the technique offers similar capabilities to OCT but at a significantly lower cost than the systems currently commercially available. The technology is significantly lower cost and higher resolution (1.5  $\mu\text{m}$  vs 10  $\mu\text{m}$ ) than the current standard, universally capable ultrasound devices. Further, the quasi-tomographic images produced by the device gives the user additional qualitative information to ease correct interpretation. The biggest disadvantage of the technique, compared to ultrasound, is due to the optical opacities of some coating layers; only clear coat and some base coat layers can be measured directly by the technique. A review of the pros and cons of LF-SD-OCR vs ultrasound has been given. To the authors' knowledge, commercially available devices and techniques with this capability are much more expensive and complex than the technique presented here. In addition, the technique may be applied in other fields involving thin layers, such as the manufacture of plastic film.

## Acknowledgments

Part of the direct funding of this work was provided by the University of Liverpool, Department of Eye and Vision Science, Post-doctoral Career Development award to Samuel Lawman. Further funding and the work which this study developed out was provided by NIHR i4i projects II-LA-0813-20005 and II-LA-1116-20008.

The Ultrasensitive Optical Coherence Tomography Imaging for Eye Disease is funded by the National Institute

for Health Research's i4i Programme. This paper summarises independent research funded by the National Institute for Health Research (NIHR) under its i4i Programme (Grant No. II-LA-1116-20008). The views expressed are those of the authors and not necessarily those of the NHS, the NIHR or the Department of Health and Social Care.

## ORCID iD

Samuel Lawman  <https://orcid.org/0000-0003-2695-4366>

## References

- [1] Bull S and Jones A A 1996 Multilayer coatings for improved performance *Surf. Coat. Technol.* **78** 173–84
- [2] Akafuah N K *et al* 2016 Evolution of the automotive body coating process—a review *Coatings* **6**
- [3] Hayes G E 1976 *Quality Assurance: Management & Technology* 2nd edn (Capistrano Beach, CA: Charger Productions)
- [4] ISO 9001:2015 2015 *Sections 8.1 d), 8.5.1 c) and 8.6 a) BS EN* (International Organization for Standardization)
- [5] Brasunas J C, Cusham G M and Lakew B 2014 Thickness measurement *The Measurement Instrumentation and Sensors Handbook* 2nd edn, ed J G Webster and H Eren (Boca Raton, FL: CRC Press)
- [6] Cole-Parmer Ltd 2019 DeFelsko Positector 200b1 coating thickness gauge non-metals 0. 5-40mils (<https://www.coleparmer.co.uk/i/defelsko-positector-200b1-coating-thickness-gauge-non-metals-0-5-40-mils/5978402>) (Accessed: 11 November 2019)
- [7] Wells B DeFelsko Corporation, Private communication 28 June 2019
- [8] Quote ID: Q7005 Imaginant Inc., Private communication 8 March 2017
- [9] Hibbard R Imaginant Inc., Private communication 28 June 2019
- [10] Green R EJr 2004 Non-contact ultrasonic techniques *Ultrasonics* **42** 9–16
- [11] Lawman S and Liang H 2011 High precision dynamic multi-interface profilometry with optical coherence tomography *Appl. Opt.* **50** 6039–48
- [12] Lawman S *et al* 2017 Applications of optical coherence tomography in the non-contact assessment of automotive paints *Proc. SPIE* accepted.
- [13] Dong Y *et al* 2016 Nondestructive analysis of automotive paints with spectral domain optical coherence tomography *Appl. Opt.* **55** 3695–700
- [14] Zhang J *et al* 2017 Non-destructive analysis of flakes in automotive paints with time-domain full-field optical coherence tomography *Optics Express* **25** 18614–28
- [15] Lawman S *et al* 2017 Scan-less line field optical coherence tomography, with automatic image segmentation as a measurement tool for automotive coatings *Appl. Sci.* **7** 351
- [16] Thorlabs Inc. 2019 OCT Imaging Systems & Components ([https://www.thorlabs.de/navigation.cfm?guide\\_id=2039](https://www.thorlabs.de/navigation.cfm?guide_id=2039)) (Accessed: 19 November 2019)
- [17] Akca B *et al* 2013 Miniature spectrometer and beam splitter for an optical coherence tomography on a silicon chip *Opt. Express* **21** 16648–56
- [18] Kim S *et al* 2018 Design and implementation of a low-cost, portable OCT system *Biomed. Opt. Express* **9** 1232–43
- [19] Song G *et al* 2019 First clinical application of low-cost OCT *Transl. Vis. Sci. Technol.* **8** 61
- [20] Subhash H M Hogan J N and Leahy M J 2015 Multiple-reference optical coherence tomography for smartphone applications *SPIE Newsroom* pp 10–12
- [21] Miller D A 2008 *Optical Properties of Solid Thin Films by Spectroscopic Reflectometry and Spectroscopic Ellipsometry* (Ann Arbor, MI: ProQuest)
- [22] Chalmers S A 2001 Rapid and accurate thin film measurement of individual layers in a multi-layered or patterned sample *US Patent* 6204922 B1
- [23] Lu H *et al* 2014 Tear film measurement by optical reflectometry technique *J. Biomed. Opt.* **19** 8
- [24] Molesini G *et al* 1984 Focus-wavelength encoded optical profilometer *Opt. Commun.* **49** 229–33
- [25] Lyda W *et al* 2012 Advantages of chromatic-confocal spectral interferometry in comparison to chromatic confocal microscopy *Meas. Sci. Technol.* **23** 054009
- [26] Boettcher T, Gronle M and Osten W 2017 Multi-layer topography measurement using a new hybrid single-shot technique: chromatic confocal coherence tomography (CCCT) *Opt. Express* **25** 10204–13
- [27] Zuluaga A F and Richards-Kortum R 1999 Spatially resolved spectral interferometry for determination of subsurface structure *Opt. Lett.* **24** 519–21
- [28] Dubey S K *et al* 2007 Fingerprint detection using full-field swept-source optical coherence tomography *Appl. Phys. Lett.* **91** 181106
- [29] Hillmann D *et al* 2017 Off-axis reference beam for full-field swept-source OCT and holoscopy *Opt. Express* **25** 27770–84
- [30] Nguyen T-U *et al* 2013 Snapshot 3D optical coherence tomography system using image mapping spectrometry *Opt. Express* **21** 13758–72
- [31] Shen Y *et al* 2017 Optical interferometry apparatus and method WO 2017/168181 A1
- [32] Williams D *et al* 2015 Fast segmentation of anterior segment optical coherence tomography images using graph cut *Eye Vision* **2** 1
- [33] Lawman S *et al* 2017 Deformation velocity imaging using optical coherence tomography and its applications to the cornea *Biomed. Opt. Express* **8** 5579–93
- [34] Lawman S *et al* 2016 High resolution corneal and single pulse imaging with line field spectral domain optical coherence tomography *Opt. Express* **24** 2395–405
- [35] Abdel-Bary E M 2003 *Handbook of Plastic Films* (Shrewsbury: iSmithers Rapra Publishing)